4-2011

Two-Stepping into the Icehouse: East Antarctic Weathering During Progressive Ice-Sheet Expansion at the Eocene–Oligocene Transition

Howie Scher
University of South Carolina - Columbia, hscher@geol.sc.edu

Steven M. Bohaty
University of California - Santa Cruz

James C. Zachos
University of California - Santa Cruz

Margaret L. Delaney
University of California - Santa Cruz

Publication Info

Two-stepping into the icehouse: East Antarctic weathering during progressive ice-sheet expansion at the Eocene–Oligocene transition

Howie D. Scher[1]*, Steven M. Bohaty[2]†, James C. Zachos[2], and Margaret L. Delaney[1]
[1]Ocean Sciences Department, and Institute of Marine Sciences, University of California–Santa Cruz, Santa Cruz, California 95064, USA
[2]Earth and Planetary Sciences Department, and Institute of Marine Sciences, University of California–Santa Cruz, Santa Cruz, California 95064, USA

ABSTRACT

In conjunction with increasing benthic foraminiferal $\delta^{18}O$ values at the Eocene–Oligocene transition (EOT; ca. 34 Ma), coarse-grained ice-rafted debris (IRD; >425 µm) appears abruptly alongside fossil fish teeth with continentally derived neodymium (Nd) isotope ratios (ε_{Nd}) in Kerguelen Plateau (Southern Ocean) sediments. Increased Antarctic weathering flux, as inferred from two steps to less radiogenic ε_{Nd} values, coincides with two steps in benthic foraminiferal $\delta^{18}O$ values. These results indicate that two distinct surges of weathering were generated by East Antarctic ice growth during the EOT. Weathering by ice sheets during a precursor glaciation at 33.9 Ma did not produce significant IRD accumulation during the first ε_{Nd} shift. Glacial weathering was sustained during a terrace interval between the two steps, probably by small high-elevation ice sheets. A large increase in weathering signals the rapid coalescence of small ice sheets into an ice sheet of continental proportions ca. 33.7 Ma. Rapid ice sheet expansion resulted in a suppression of weathering due to less exposed area and colder conditions. Parallel changes in Antarctic weathering flux and deep-sea carbonate accumulation suggest that ice-sheet expansion during the EOT had a direct impact on the global carbon cycle; possible mechanisms include associated changes in silicate weathering on the East Antarctic craton and enhanced fertilization of Southern Ocean waters, both of which warrant further investigation.

INTRODUCTION

The sudden appearance of ice sheets on Antarctica during the Eocene–Oligocene transition (EOT) produced a surge of erosion that carried weathering products to depocenters around the circum-Antarctic. Remnants of this weathering event are found in Early Oligocene strata as glaciomarine sequences on the continental shelves (Cooper and O'Brien, 2004) and as coarse grains of ice-rafted debris (IRD) in pelagic sediments (Zachos et al., 1992). A shift from smectite- to illite-dominated clay mineral assemblages signals the transition from a chemical weathering regime on Antarctica to one of mechanical weathering by ice sheets (Ehrmann and Mackensen, 1992). However, knowledge of the timing and magnitude of weathering and IRD deposition in the Early Oligocene is limited compared to cooling and/or ice volume increase history gleaned from deep-sea benthic foraminiferal $\delta^{18}O$ records, which reveal a two-step transition from greenhouse to icehouse climate (Coxall et al., 2005).

Radiogenic isotopes of long-lived radioactive systems are excellent paleoceanographic proxies for continental weathering (e.g., Armstrong, 1971) because of the great isotopic disparity between mantle-derived and continental sources (e.g., Zachos et al., 1999; Dalai et al., 2006). Seawater neodymium (Nd) is almost exclusively derived from continental weathering (e.g., van de Flierdt et al., 2007) and has a short residence time (500–1000 yr) compared to the duration of the EOT (~200 k.y.). Fossil fish teeth in pelagic sediments take up large amounts of Nd during early diagenesis (Bernat, 1975). Rates of postburial Nd uptake (e.g., Kocsis et al., 2010) are very low relative to early diagenetic rare earth element (REE) uptake in oxidizing pelagic sediments (e.g., Staudigel et al., 1985; C. Trueman, 2010, personal commun.), permitting retention of bottom-water ε_{Nd} values (e.g., Martin and Haley, 2000). Thus, changes in fossil fish tooth ε_{Nd} records from sediment cores near Antarctica are likely to preserve a signal of Nd carried with the weathering surge in the EOT interval. The objectives of this study are to determine the signal of Antarctic weathering and evaluate the timing of weathering changes relative to IRD deposition and cooling and ice volume proxies across the EOT.

The ε_{Nd} values reflect the $^{143}Nd/^{144}Nd$ ratio relative to bulk Earth, where ε_{Nd} values of continental crust become less radiogenic (i.e., negative) with older mantle extraction ages (DePaolo and Wasserburg, 1976). Low-resolution Nd isotope records reveal anomalously low ε_{Nd} values for Southern Ocean waters at 34 Ma (Scher and Martin, 2004, 2006), indicating a source of non-

radiogenic Nd (i.e., typical of ancient continental crust). Low ε_{Nd} values at the EOT could be a signal of Antarctic glacial weathering (Scher and Martin, 2004). Precambrian basement, including Archean terranes in Prydz Bay (Fitzsimons, 2003), outcrops in East Antarctica (Fig. 1A), contributing sediment with extremely nonradiogenic Nd to Prydz Bay and areas around the Kerguelen Plateau (Fig. 1B; Roy et al., 2007; van de Flierdt et al., 2007). These terranes are the likely source of low ε_{Nd} values measured in Late Eocene glaciomarine sediments within Prydz Bay (van de Flierdt et al., 2008).

MATERIAL AND METHODS

We developed coupled records of benthic foraminiferal $\delta^{18}O$, fossil fish tooth ε_{Nd}, and IRD concentrations from the EOT interval of Ocean
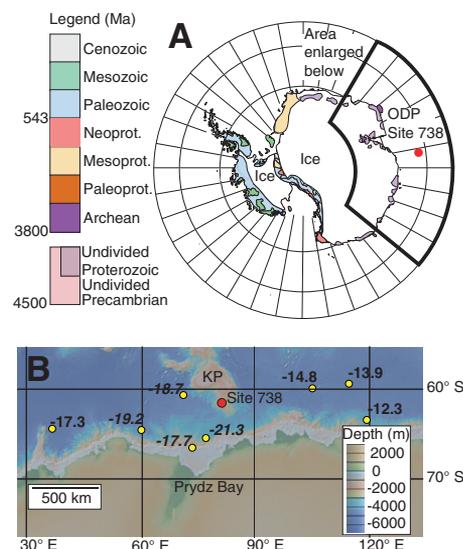
Figure 1. A: Antarctic outcrops with colors corresponding to geological age (prot.—Proterozoic), modified from Roy et al. (2007), and position of Ocean Drilling Program (ODP) Site 738 (red dot; 62°43′S, 82°47′E, 2253 m water depth, 1750 m EOT [Eocene–Oligocene transition] paleodepth). B: Detrital ε_{Nd} values from circum-Antarctic core-top samples (yellow dots) (Roy et al., 2007; van de Flierdt et al., 2007) and study site (red dot). The least radiogenic ε_{Nd} values (i.e., lowest) in the circum-Antarctic are found in the Prydz Bay sector; they average −21 ε_{Nd} (average of values in italics) and reflect ancient sediment sources in East Antarctica and within Prydz Bay (shown in A).

Drilling Program (ODP) Site 738 (Fig. 2). ODP Hole 738B was sampled at an average interval of 11 cm between ~18.0 and 29.5 m below seafloor (total 99 samples), spanning the interval between 34.1 and 33.4 Ma on our age model. Details for analytical methods and the age model are given in the GSA Data Repository.[1]

RESULTS

The $\delta^{18}O$ record for Site 738 derived from the benthic foraminifera *Cibicidoides praemundulus* reveals a two-step pattern (Fig. 2, left panel), similar to that found by Coxall et al. (2005) at ODP Site 1218 in the equatorial Pacific. The first step occurs ca. 33.9 Ma and the second, larger, step occurs ca. 33.7 Ma. An interval of intermediate and relatively uniform $\delta^{18}O$ values produces a terrace between the two prominent steps (33.9–33.7 Ma).

The primary feature of the fossil fish tooth Nd isotope record is a two-stage excursion to less radiogenic ε_{Nd} values (Fig. 2, center). During the preexcursion interval (34.5–33.9 Ma), ε_{Nd} values average −7.3. The excursion interval (33.9–33.6 Ma) begins with a step decrease of 0.7 ε_{Nd} that coincides with the first $\delta^{18}O$ step. The first Nd isotope step is followed by an ~150 k.y. interval of uniform ε_{Nd} values, similar to the $\delta^{18}O$ terrace interval. The ε_{Nd} terrace ends abruptly with a second, larger step decrease of 2.1 ε_{Nd} at 33.75 Ma that coincides with the

second $\delta^{18}O$ step. The nadir of the excursion is −10.2 ε_{Nd} at 33.7 Ma, which is followed by an ~130 k.y. recovery interval to higher values. The ε_{Nd} values in the postexcursion interval (33.6–33.3 Ma) average −8.0.

The first significant occurrence of IRD appears ~30 cm above the onset of the second step in $\delta^{18}O$ and ε_{Nd} values, in a thin stratigraphic horizon (~50 cm thick) (Fig. 2, right). IRD concentrations and mass accumulation rates reach peak values for ~75 k.y. centered ca. 33.7 Ma.

Individual fish teeth, including six samples from within the IRD horizon, show similar shale-normalized rare earth element and yttrium (REE + Y) profiles (Fig. 3). All of the patterns exhibit prominent cerium (Ce) and Y anomalies, which are diagnostic features of seawater (German and Elderfield, 1990; Nozaki et al., 1997). Furthermore, samples in this study define a relationship of Ce versus Y anomalies that is inconsistent with mixing between oxic seawater and continental crust (see the Data Repository), making postburial uptake of IRD-derived REE + Y by fossil fish teeth unlikely.

DISCUSSION

Timing of IRD Delivery to the Kerguelen Plateau

The record of IRD accumulation at Site 738 indicates that grains were delivered to the Ker-

guelen Plateau during a short episode of ice rafting (<75 k.y.), consistent with earlier studies (Zachos et al., 1992). The coincidence of peak IRD accumulation with the second larger $\delta^{18}O$ step indicates rapid, large-scale ice sheet expansion. However, no significant ice rafting was associated with the first $\delta^{18}O$ step of the EOT or with the earliest Oligocene glacial maximum (EOGM; Liu et al., 2004).

Nature of the Nd Isotope Excursion

The Nd isotope excursion begins slightly before the onset of IRD deposition (ca. 33.7 Ma), a strong indication that both are related to a single process. Variations in bottom-water ε_{Nd} values reflect changes in water mass mixing and the weathering flux to the water mass source region. If late-stage diagenesis is not an issue, coherence between IRD and ε_{Nd} records can be interpreted in two ways. One is a shift in ocean circulation coincident with the expansion of ice sheets during the second step of the EOT. Alternatively, the Nd isotope excursion could reflect an increase in the dissolved weathering flux entering the source area of the water mass bathing the upper Kerguelen Plateau. Here we evaluate the likelihood of each of these interpretations.

The least radiogenic water mass during the EOT was in the North Atlantic (ε_{Nd} = −11; O'Nions et al., 1998). Northern Component Water (NCW) was exported into the South Atlantic and Southern Ocean during the Oligocene (Scher and Martin, 2008; Via and Thomas, 2006). However, mass balance indicates that the unlikely mixture of 78% NCW at ~63°S in the Indian sector of the Southern Ocean would have been required to produce the observed excursion. With the same parameters, 18% of NCW is required to produce the initial, smaller ε_{Nd}
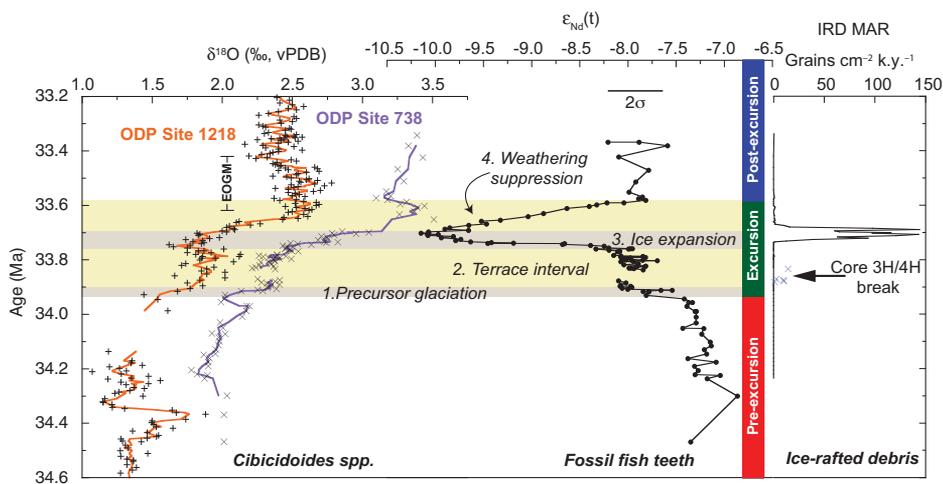
Figure 2. Ocean Drilling Program (ODP) Site 738 $\delta^{18}O$, Nd isotope, and ice-rafted debris (IRD) mass accumulation rates (MAR) records versus age. Vertical bar illustrates trends in ε_{Nd} record that define preexcursion (red), excursion (green), and postexcursion (blue) intervals. Four phases of ice sheet growth and/or weathering discussed in text are labeled. Anomalous IRD grains (marked by X) that occur at the 738B-3H/4H core break are most likely due to contamination resulting from the coring process. Nd isotope results have been normalized to the La Jolla standard = 0.511858. Error bar reflects long-term reproducibility based on replicate analysis of Ames Nd standard. Benthic foraminiferal $\delta^{18}O$ record from ODP Site 1218 is from Coxall et al. (2005). All $\delta^{18}O$ results have been adjusted by +0.64‰. EOGM—earliest Oligocene glacial maximum.
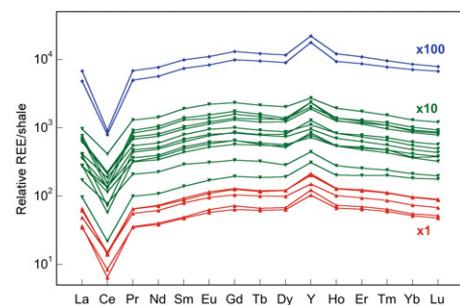
Figure 3. Shale-normalized rare earth element and yttrium (REE + Y) concentrations of fossil fish teeth used in this study normalized to post-Archean Australian Shale (PAAS) using values from Taylor and McLennan (1985). Normalized concentrations of samples taken from preexcursion (red), excursion (green), and postexcursion (blue) intervals have been adjusted by factors of 10 (1, 10, and 100, respectively) to enable visual comparison. Prominent Ce and Y anomalies are present in samples from each interval.

step. However, ε_{Nd} values at 42°S in the southern Atlantic (ODP Site 1090; Scher and Martin, 2006) only shift by 0.6 ε_{Nd} across the first $\delta^{18}O$ step (~251 m composite depth). Thus it is more likely that the source of nonradiogenic ε_{Nd} values during the first step was in closer proximity to the Kerguelen Plateau than to the Agulhas Ridge, which argues against an influx of NCW as the source of the excursion.

Mechanical erosion of Antarctic bedrock by ice sheets followed by rapid chemical breakdown of fresh mineral surfaces would have released extremely nonradiogenic Nd into the dissolved load accompanying the weathering surge during ice sheet growth. However, the delivery of Nd from Antarctic sources to bottom waters on the Kerguelen Plateau in pulses that are coeval with the benthic foraminiferal $\delta^{18}O$ steps requires the combined operation of three transport vectors: (1) production of fine-grained material with freshly exposed mineral surfaces during ice sheet expansion, (2) rapid chemical breakdown of fresh surfaces during transport within the Prydz Bay drainage system, and (3) rapid mixing of dissolved nonradiogenic Nd from the Antarctic weathering flux with interior ocean water masses. The first and second transport processes are based on two tenets of glaciological theory: freshly exposed mineral surfaces undergo rapid chemical breakdown during transport (Anderson, 2007), and production of fine-grained sediment is as much as 10 times higher in glaciated catchments relative to nonglaciated ones (Hallet et al., 1996).

Operation of the third process is indicated by REE behavior in the modern ocean. REEs are scavenged in low-salinity regions of estuaries through colloidal flocculation and released in higher salinity regions (Sholkovitz, 1992, 1993), where they mix with shelf waters. Today, Antarctic Bottom Water (AABW) forms along the Antarctic shelf to the east of Prydz Bay (Orsi et al., 1999), and is detectable below 4000 m in the Australian-Antarctic basin (van de Flierdt et al., 2006). The Kerguelen Deep Western Boundary Current (DWBC) exports AABW at depths below 2500 m along the eastern flank of the plateau (Fukamachi et al., 2010). The paleodepth of the study site (~1750 m) was 750 m shallower than the present-day depth of AABW in the DWBC; however, the ε_{Nd} signal may have migrated upward via mixing. Alternatively, the study site may have been influenced by local and/or regional production of an intermediate or deep-water mass on the Antarctic shelves.

Weathering and Ice Volume History Across the EOT

Our IRD and ε_{Nd} records enable a detailed reconstruction of continental weathering during early ice sheet expansion on East Antarctica. Changes in weathering during the excursion interval occurred in four phases (Fig. 2). During phase 1, the flux of nonradiogenic Nd increased in conjunction with the first $\delta^{18}O$ step, indicating that ice sheets formed at 33.9 Ma, here called the precursor glaciation. The ε_{Nd} signal in this interval resulted from the interplay of mechanical and chemical weathering, as described above, and is consistent with the initial appearance of illite-dominated clay mineral assemblages on the Kerguelen Plateau (ca. 33.9 Ma; Ehrmann and Mackensen, 1992), coincident with the first $\delta^{18}O$ and ε_{Nd} steps. The early ice sheets were probably restricted to high interior elevations (e.g., DeConto and Pollard, 2003) and thus incapable of rafting icebergs, explaining the lack of IRD during the first $\delta^{18}O$ and ε_{Nd} steps. A precursor glaciation that coincides with the first $\delta^{18}O$ and ε_{Nd} step is compatible with recent estimates of changes in sea level across the first step (Katz et al., 2008).

Phase 2 is the terrace interval of relatively uniform ε_{Nd} values between the two steps. It is noteworthy that the duration of sustained negative ε_{Nd} values (~150 k.y.) is much longer than the residence time of Nd, requiring an ongoing flux of nonradiogenic Nd. This strongly indicates that the relatively stable small- to medium-sized ice sheets nonetheless advanced and retreated on orbital time scales, thus maintaining a supply of freshly weathered mineral surfaces for chemical weathering. This finding supports the ice sheet hysteresis hypothesis related to the height–mass balance feedback modeled by Pollard and DeConto (2005); i.e., once formed, high-elevation ice sheets are stable because the ice surface is above the zone of ablation, which is strongly controlled by atmospheric CO_2 levels.

It is possible that Antarctic weathering during the terrace interval contributed to lower CO_2 through two mechanisms. The first is nutrient delivery to the Southern Ocean supplied by enhanced weathering and vertical mixing (i.e., intensification of polar easterlies) and increased primary productivity, indicated by increased opal accumulation (Salamy and Zachos, 1999). Second, enhanced silicate weathering (Berner et al., 1983) in East Antarctica during this intermediate phase of limited glaciation may have acted as a positive feedback to cooling on EOT time scales (i.e., by increasing the silicate weathering CO_2 sink). Estimates of surface ocean pH from Tanzanian drill cores suggest that CO_2 was relatively low toward the end of the terrace interval (Pearson et al., 2009), supporting the argument that ice sheet weathering feedbacks helped sustain EOT climate change. Parallel changes between Antarctic weathering flux and calcite compensation depth deepening (e.g., Rea and Lyle, 2005) further indicate that weathering was an important factor for global carbon cycling in this interval.

During phase 3, a massive and abrupt increase in weathering flux occurred as the precursor ice sheets coalesced and expanded to cover the East Antarctic craton. Comparison of ε_{Nd} and IRD records shows that the dissolved weathering flux carried in proglacial rivers reached the sea slightly before IRD reached the Kerguelen Plateau. During phase 4, coinciding with the EOGM, rates of mechanical and chemical weathering slowed as temperatures dropped, liquid water became scarce, and weatherable area diminished. It is likely that these factors contributed to the termination of IRD deposition at the study site during the earliest Oligocene glacial maximum.

Over the recovery interval to higher ε_{Nd} values, the impact of chemical weathering on Antarctica as a sink for CO_2 diminished, permitting CO_2 to build up in the atmosphere (e.g., Pearson et al., 2009). Zachos and Kump (2005) modeled the climate response of decreasing Antarctic weatherability as a function of ice coverage and found that the CO_2 response could explain the warming trend that ended the earliest Oligocene glacial maximum. Results from our study provide partial support of this hypothesis, demonstrating that a decrease in weathering accompanied the final build-up and maximum extent of the East Antarctic ice sheet during the Early Oligocene.

CONCLUSIONS

A detailed weathering history of East Antarctica during the EOT has been reconstructed on the basis of IRD MAR and ε_{Nd} values from fossil fish teeth at ODP Site 738 on the Kerguelen Plateau. These tracers of terrigenous input track two extremes in the size spectrum of glacially weathered products that reach the pelagic realm: mechanically weathered coarse grains transported by drifting icebergs and chemically weathered dissolved solutes transported by proglacial rivers. We show for the first time that two distinct weathering pulses occurred during the EOT, simultaneous with two benthic foraminiferal $\delta^{18}O$ steps. Ice sheets formed in the latest Eocene (33.9 Ma) were limited to elevated regions and did not reach sea level, but persisted throughout the terrace interval until the second step. The large ice sheet that formed suddenly at 33.7 Ma quickly reduced the weatherable area on Antarctica, resulting in a weathering flux decline, with effects on the progression of global climate change during the Early Oligocene.

REFERENCES CITED

Anderson, S.P., 2007, Biogeochemistry of glacial landscape systems: Annual Review of Earth and Planetary Sciences, v. 35, p. 375–399, doi: 10.1146/annurev.earth.35.031306.140033.

Armstrong, R.L., 1971, Glacial erosion and the variable isotopic composition of strontium in seawater: Nature, v. 230, p. 132–134.

Berner, R.A., Lasaga, A.C., and Garrels, R.M., 1983, The carbonate-silicate geochemical cycle and its effects on atmospheric carbon dioxide over the past 100 million years: American Journal of Science, v. 283, p. 641–683, doi: 10.2475/ajs.283.7.641.

Cooper, A.K., and O'Brien, P.E., 2004, Leg 188 synthesis: Transitions in the glacial history of the Prydz Bay region, East Antarctica, from ODP drilling, in Cooper, A.K., et al., eds., Proceedings of the Ocean Drilling Program, Scientific results, Volume 188: College Station, Texas, Ocean Drilling Program, p. 1–42, http://www-odp.tamu.edu/publications/188_SR/VOLUME/SYNTH/SYNTH.PDF.

Coxall, H.K., Wilson, P.A., Pälike, H., Lear, C.H., and Backman, J., 2005, Rapid stepwise onset of Antarctic glaciation and deeper calcite compensation in the Pacific Ocean: Nature, v. 433, p. 53–57, doi: 10.1038/nature03135.

Dalai, T.K., Ravizza, G.E., and Peucker-Ehrenbrink, B., 2006, The Late Eocene $^{187}Os/^{188}Os$ excursion: Chemostratigraphy, cosmic dust flux and the Early Oligocene glaciation: Earth and Planetary Science Letters, v. 241, p. 477–492, doi: 10.1016/j.epsl.2005.11.035.

DeConto, R.M., and Pollard, D., 2003, Rapid Cenozoic glaciation of Antarctica induced by declining atmospheric CO_2: Nature, v. 421, p. 245–249, doi: 10.1038/nature01290.

DePaolo, D.J., and Wasserburg, G.J., 1976, Nd isotopic variations and petrogenetic models: Geophysical Research Letters, v. 3, p. 249–252, doi: 10.1029/GL003i005p00249.

Ehrmann, W.U., and Mackensen, A., 1992, Sedimentological evidence for the formation of an East Antarctic ice sheet in Eocene/Oligocene time: Palaeogeography, Palaeoclimatology, Palaeoecology, v. 93, p. 85–112, doi: 10.1016/0031-0182(92)90185-8.

Fitzsimons, I.C.W., 2003, Proterozoic basement provinces of southern and southwestern Australia, and their correlation with Antarctica, in Yoshida, M., et al., eds., Proterozoic East Gondwana: Supercontinent assembly and breakup: Geological Society of London Special Publication 206, p. 93–130 doi: 10.1144/GSL.SP.2003.206.01.07.

Fukamachi, Y., Rintoul, S.R., Church, J.A., Aoki, S., Sokolov, S., Rosenberg, M.A., and Wakatsuchi, M., 2010, Strong export of Antarctic Bottom Water east of the Kerguelen plateau: Nature Geoscience, v. 3, p. 327–331, doi: 10.1038/ngeo842.

German, C.R., and Elderfield, H., 1990, Application of the Ce anomaly as a paleoredox indicator: The ground rules: Paleoceanography, v. 5, p. 823–833, doi: 10.1029/PA005i005p00823.

Hallet, B., Hunter, L., and Bogen, J., 1996, Rates of erosion and sediment evacuation by glaciers: A review of field data and their implications: Global and Planetary Change, v. 12, p. 213–235, doi: 10.1016/0921-8181(95)00021-6.

Katz, M.E., Miller, K.G., Wright, J.D., Wade, B.S., Browning, J.V., Cramer, B.S., and Rosenthal, Y., 2008, Stepwise transition from the Eocene greenhouse to the Oligocene icehouse: Nature Geoscience, v. 1, p. 329–334, doi: 10.1038ngeo179.

Kocsis, L., Trueman, C.N., and Palmer, M.R., 2010, Protracted diagenetic alteration of REE contents in fossil bioapatites: Direct evidence from Lu-Hf isotope systematics: Geochimica et Cosmochimica Acta, v. 74, p. 6077–6092, doi: 10.1016/j.gca.2010.08.007.

Liu, Z.F., Tuo, S.T., Zhao, Q.H., Cheng, X.R., and Huang, W., 2004, Deep-water earliest Oligocene glacial maximum (EOGM) in South Atlantic: Chinese Science Bulletin, v. 49, p. 2190–2197, doi: 10.1360/04wd0228.

Martin, E.E., and Haley, B.A., 2000, Fossil fish teeth as proxies for seawater Sr and Nd isotopes: Geochimica et Cosmochimica Acta, v. 64, p. 835–847, doi: 10.1016/S0016-7037(99)00376-2.

Nozaki, Y., Zhang, J., and Amakawa, H., 1997, The fractionation between Y and Ho in the marine environment: Earth and Planetary Science Letters, v. 148, p. 329–340, doi: 10.1016/S0012-821X(97)00034-4.

O'Nions, R.K., Frank, M., von Blanckenburg, F., and Ling, H.F., 1998, Secular variation of Nd and Pb isotopes in ferromanganese crusts from the Atlantic, Indian and Pacific Oceans: Earth and Planetary Science Letters, v. 155, p. 15–28, doi: 10.1016/S0012-821X(97)00207-0.

Orsi, A.H., Johnson, G.C., and Bullister, J.L., 1999, Circulation, mixing, and production of Antarctic Bottom Water: Progress in Oceanography, v. 43, p. 55–109, doi: 10.1016/S0079-6611(99)00004-X.

Pearson, P.N., Foster, G.L., and Wade, B.S., 2009, Atmospheric carbon dioxide through the Eocene-Oligocene climate transition: Nature, v. 461, p. 1110–1113, doi: 10.1038/nature08447.

Pollard, D., and DeConto, R.M., 2005, Hysteresis in Cenozoic Antarctic ice-sheet variations: Global and Planetary Change, v. 45, p. 9–21, doi: 10.1016/j.gloplacha.2004.09.011.

Rea, D.K., and Lyle, M.W., 2005, Paleogene calcite compensation depth in the eastern subtropical Pacific: Answers and questions: Paleoceanography, v. 20, PA1012, doi: 10.1029/2004PA001064.

Roy, M., van de Flierdt, T., Hemming, S.R., and Goldstein, S.L., 2007, $^{40}Ar/^{39}Ar$ ages of hornblende grains and bulk Sm/Nd isotopes of circum-Antarctic glacio-marine sediments: Implications for sediment provenance in the Southern Ocean: Chemical Geology, p. 507–519, doi: 10.1016/j.chemgeo.2007.07.017.

Salamy, K.A., and Zachos, J.C., 1999, Latest Eocene–Early Oligocene climate change and Southern Ocean fertility: Inferences from sediment accumulation and stable isotope data: Palaeogeography, Palaeoclimatology, Palaeoecology, v. 145, p. 61–77, doi: 10.1016/S0031-0182(98)00093-5.

Scher, H.D., and Martin, E.E., 2004, Circulation in the Southern Ocean during the Paleogene inferred from neodymium isotopes: Earth and Planetary Science Letters, v. 228, p. 391–405, doi: 10.1016/j.epsl.2004.10.016.

Scher, H.D., and Martin, E.E., 2006, Timing and climatic consequences of the opening of Drake Passage: Science, v. 312, p. 428–430, doi: 10.1126/science.1120044.

Scher, H.D., and Martin, E.E., 2008, Oligocene deep water export from the North Atlantic and the development of the Antarctic Circumpolar Current examined with neodymium isotopes: Paleoceangraphy, v. 23, PA1205, doi: 10.1029/2006PA001400.

Sholkovitz, E.R., 1992, Chemical evolution of rare-earth elements—Fractionation between colloidal and solution phases of filtered river water: Earth and Planetary Science Letters, v. 114, p. 77–84, doi: 10.1016/0012-821X(92)90152-L.

Sholkovitz, E.R., 1993, The geochemistry of rare earth elements in the Amazon River estuary: Geochimica et Cosmochimica Acta, v. 57, p. 2181–2190, doi: 10.1016/0016-7037(93)90559-F.

Staudigel, H., Doyle, P., and Zindler, A., 1985, Sr and Nd isotope systematics in fish teeth: Earth and Planetary Science Letters, v. 76, p. 45–56, doi: 10.1016/0012-821X(85)90147-5.

Taylor, S.R., and McLennan, S.M., 1985, The continental crust: Its composition and evolution: Oxford, UK, Blackwell Scientific Publications, 312 p.

van de Flierdt, T., Hemming, S.R., Goldstein, S.L., and Abouchami, W., 2006, Radiogenic isotope fingerprint of Wilkes Land–Adélie Coast Bottom Water in the circum-Antarctic Ocean: Geophysical Research Letters, v. 33, L12606, doi: 10.1029/2006GL026020.

van de Flierdt, T., Goldstein, S.L., Hemming, S.R., Roy, M., Frank, M., and Halliday, A.N., 2007, Global neodymium-hafnium isotope systematics—Revisited: Earth and Planetary Science Letters, v. 259, p. 432–441, doi: 10.1016/j.epsl.2007.05.003.

van de Flierdt, T., Hemming, S.R., Goldstein, S.L., Gehrels, G.E., and Cox, S.E., 2008, Evidence against a young volcanic origin of the Gamburtsev Subglacial Mountains, Antarctica: Geophysical Research Letters, v. 35, L21303, doi: 10.1029/2008GL035564.

Via, R.K., and Thomas, D.J., 2006, Evolution of Atlantic thermohaline circulation: Early Oligocene onset of deep-water production in the North Atlantic: Geology, v. 34, p. 441–444, doi: 10.1130/G22545.1.

Zachos, J.C., and Kump, L.R., 2005, Carbon cycle feedbacks and the initiation of Antarctic glaciation in the earliest Oligocene: Global and Planetary Change, v. 47, p. 51–66, doi: 10.1016/j.gloplacha.2005.01.001.

Zachos, J.C., Breza, J., and Wise, S.W., 1992, Early Oligocene ice-sheet expansion on Antarctica: Stable isotope and sedimentological evidence from Kerguelen Plateau, southern Indian Ocean: Geology, v. 20, p. 569–573, doi: 10.1130/0091-7613(1992)020<0569:EOISEO>2.3.CO;2.

Zachos, J.C., Opdyke, B.N., Quinn, T.M., Jones, C.E., and Halliday, A.N., 1999, Early Cenozoic glaciation, Antarctic weathering, and seawater $^{87}Sr/^{86}Sr$: Is there a link?: Chemical Geology, v. 161, p. 165–180, doi: 10.1016/S0009-2541(99)00085-6.